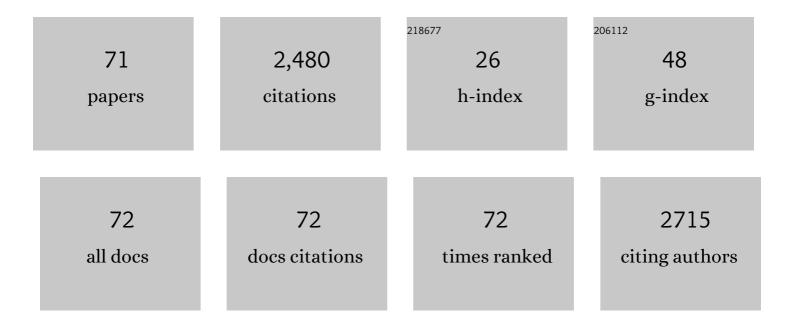
Takazo Shibuya

List of Publications by Year in descending order

Source: https://exaly.com/author-pdf/9746622/publications.pdf Version: 2024-02-01



#	Article	IF	CITATIONS
1	Ongoing hydrothermal activities within Enceladus. Nature, 2015, 519, 207-210.	27.8	382
2	The Drive to Life on Wet and Icy Worlds. Astrobiology, 2014, 14, 308-343.	3.0	232
3	High-temperature water–rock interactions and hydrothermal environments in the chondrite-like core of Enceladus. Nature Communications, 2015, 6, 8604.	12.8	152
4	Geological background of the Kairei and Edmond hydrothermal fields along the Central Indian Ridge: Implications of their vent fluids' distinct chemistry. Geofluids, 2008, 8, 239-251.	0.7	112
5	Evolution of the composition of seawater through geologic time, and its influence on the evolution of life. Gondwana Research, 2008, 14, 159-174.	6.0	91
6	Highly alkaline, high-temperature hydrothermal fluids in the early Archean ocean. Precambrian Research, 2010, 182, 230-238.	2.7	88
7	Discovery of New Hydrothermal Activity and Chemosynthetic Fauna on the Central Indian Ridge at 18°–20°S. PLoS ONE, 2012, 7, e32965.	2.5	83
8	Diversity of fluid geochemistry affected by processes during fluid upwelling in active hydrothermal fields in the Izena Hole, the middle Okinawa Trough back-arc basin. Geochemical Journal, 2014, 48, 357-369.	1.0	69
9	The youngest blueschist belt in SW Japan: implication for the exhumation of the Cretaceous Sanbagawa highâ€≺i>P/T metamorphic belt. Journal of Metamorphic Geology, 2008, 26, 583-602.	3.4	63
10	Grain-scale iron isotopic distribution of pyrite from Precambrian shallow marine carbonate revealed by a femtosecond laser ablation multicollector ICP-MS technique: Possible proxy for the redox state of ancient seawater. Geochimica Et Cosmochimica Acta, 2010, 74, 2760-2778.	3.9	59
11	Reactions between basalt and CO2-rich seawater at 250 and 350 ŰC, 500 bars: Implications for the CO2 sequestration into the modern oceanic crust and the composition of hydrothermal vent fluid in the CO2-rich early ocean. Chemical Geology, 2013, 359, 1-9.	3.3	56
12	Postâ€drilling changes in fluid discharge pattern, mineral deposition, and fluid chemistry in the Iheya North hydrothermal field, Okinawa Trough. Geochemistry, Geophysics, Geosystems, 2013, 14, 4774-4790.	2.5	52
13	Free energy distribution and hydrothermal mineral precipitation in Hadean submarine alkaline vent systems: Importance of iron redox reactions under anoxic conditions. Geochimica Et Cosmochimica Acta, 2016, 175, 1-19.	3.9	52
14	Deepest and hottest hydrothermal activity in the Okinawa Trough: the Yokosuka site at Yaeyama Knoll. Royal Society Open Science, 2017, 4, 171570.	2.4	48
15	Are the Taitao granites formed due to subduction of the Chile ridge?. Lithos, 2009, 113, 246-258.	1.4	46
16	Variability in Microbial Communities in Black Smoker Chimneys at the NW Caldera Vent Field, Brothers Volcano, Kermadec Arc. Geomicrobiology Journal, 2009, 26, 552-569.	2.0	46
17	Geotectonic framework of the Blueschist Unit on Anglesey–Lleyn, UK, and its role in the development of a Neoproterozoic accretionary orogen. Precambrian Research, 2007, 153, 11-28.	2.7	45
18	Hydrogen-rich hydrothermal environments in the Hadean ocean inferred from serpentinization of komatiites at 300°C and 500Âbar. Progress in Earth and Planetary Science, 2015, 2, .	3.0	45

Τακάζο Shibuya

#	Article	lF	CITATIONS
19	Rapid growth of mineral deposits at artificial seafloor hydrothermal vents. Scientific Reports, 2016, 6, 22163.	3.3	44
20	Middle Archean ocean ridge hydrothermal metamorphism and alteration recorded in the Cleaverville area, Pilbara Craton, Western Australia. Journal of Metamorphic Geology, 2007, 25, 751-767.	3.4	42
21	Potential for biogeochemical cycling of sulfur, iron and carbon within massive sulfide deposits below the seafloor. Environmental Microbiology, 2015, 17, 1817-1835.	3.8	42
22	Genomeâ€enabled metabolic reconstruction of dominant chemosynthetic colonizers in deepâ€sea massive sulfide deposits. Environmental Microbiology, 2018, 20, 862-877.	3.8	41
23	87Sr/86Sr chemostratigraphy of Neoproterozoic Dalradian carbonates below the Port Askaig Glaciogenic Formation, Scotland. Precambrian Research, 2010, 179, 150-164.	2.7	37
24	Monazite geochronology and geochemistry of meta-sediments in the Narryer Gneiss Complex, Western Australia: constraints on the tectonothermal history and provenance. Contributions To Mineralogy and Petrology, 2010, 160, 803-823.	3.1	32
25	H2 generation by experimental hydrothermal alteration of komatiitic glass at 300°C and 500 bars: A preliminary result from on-going experiment. Geochemical Journal, 2009, 43, e17-e22.	1.0	30
26	Fluid chemistry in the Solitaire and Dodo hydrothermal fields of the Central Indian Ridge. Geofluids, 2016, 16, 988-1005.	0.7	29
27	Depth variation of carbon and oxygen isotopes of calcites in Archean altered upperoceanic crust: Implications for the CO2 flux from ocean to oceanic crust in the Archean. Earth and Planetary Science Letters, 2012, 321-322, 64-73.	4.4	27
28	Experimental and Simulation Efforts in the Astrobiological Exploration of Exooceans. Space Science Reviews, 2020, 216, 9.	8.1	25
29	Reactions between komatiite and CO2-rich seawater at 250 and 350°C, 500 bars: implications for hydrogen generation in the Hadean seafloor hydrothermal system. Progress in Earth and Planetary Science, 2016, 3, .	3.0	24
30	Nitrification-driven forms of nitrogen metabolism in microbial mat communities thriving along an ammonium-enriched subsurface geothermal stream. Geochimica Et Cosmochimica Acta, 2013, 113, 152-173.	3.9	23
31	Simulating Serpentinization as It Could Apply to the Emergence of Life Using the JPL Hydrothermal Reactor. Astrobiology, 2020, 20, 307-326.	3.0	22
32	Progressive metamorphism of the Taitao ophiolite; evidence for axial and off-axis hydrothermal alterations. Lithos, 2007, 98, 233-260.	1.4	21
33	Rock magnetism of tiny exsolved magnetite in plagioclase from a Paleoarchean granitoid in the Pilbara craton. Geochemistry, Geophysics, Geosystems, 2015, 16, 112-125.	2.5	20
34	Peptide Synthesis under the Alkaline Hydrothermal Conditions on Enceladus. ACS Earth and Space Chemistry, 2019, 3, 2559-2568.	2.7	20
35	Molecular-scale insights into differences in the adsorption of cesium and selenium on biogenic and abiogenic ferrihydrite. Geochimica Et Cosmochimica Acta, 2019, 251, 1-14.	3.9	19
36	In-situ iron isotope analyses of pyrites from 3.5 to 3.2Ga sedimentary rocks of the Barberton Greenstone Belt, Kaapvaal Craton. Chemical Geology, 2015, 403, 58-73.	3.3	17

Τακάζο Shibuya

#	Article	IF	CITATIONS
37	Decrease of seawater CO2 concentration in the Late Archean: An implication from 2.6 Ga seafloor hydrothermal alteration. Precambrian Research, 2013, 236, 59-64.	2.7	16
38	Stratigraphy-related, low-pressure metamorphism in the Hardey Syncline, Hamersley Province, Western Australia. Gondwana Research, 2010, 18, 213-221.	6.0	15
39	Petrogenesis of the ridge subduction-related granitoids from the Taitao Peninsula, Chile Triple Junction Area. Geochemical Journal, 2013, 47, 167-183.	1.0	15
40	Biological and physical modification of carbonate system parameters along the salinity gradient in shallow hypersaline solar salterns in Trapani, Italy. Geochimica Et Cosmochimica Acta, 2017, 208, 354-367.	3.9	15
41	Europium anomaly variation under low-temperature water-rock interaction: A new thermometer. Geochemistry International, 2017, 55, 822-832.	0.7	15
42	Large P–T gap between Ballantrae blueschist/garnet pyroxenite and surrounding ophiolite, southern Scotland, UK: Diapiric exhumation of a Caledonian serpentinite mélange. Lithos, 2008, 104, 337-354.	1.4	14
43	Recycled Archean sulfur in the mantle wedge of the Mariana Forearc and microbial sulfate reduction within an extremely alkaline serpentine seamount. Earth and Planetary Science Letters, 2018, 491, 109-120.	4.4	14
44	The role of hydrothermal sulfate reduction in the sulfur cycles within Europa: Laboratory experiments on sulfate reduction at 100ÂMPa. Icarus, 2021, 357, 114222.	2.5	13
45	Composition of the Primordial Ocean Just after Its Formation: Constraints from the Reactions between the Primitive Crust and a Strongly Acidic, CO2-Rich Fluid at Elevated Temperatures and Pressures. Minerals (Basel, Switzerland), 2021, 11, 389.	2.0	13
46	Authigenic carbonate precipitation at the end-Guadalupian (Middle Permian) in China: Implications for the carbon cycle in ancient anoxic oceans. Progress in Earth and Planetary Science, 2015, 2, .	3.0	11
47	Stable Abiotic Production of Ammonia from Nitrate in Komatiite-Hosted Hydrothermal Systems in the Hadean and Archean Oceans. Minerals (Basel, Switzerland), 2021, 11, 321.	2.0	10
48	Chemical Nature of Hydrothermal Fluids Generated by Serpentinization and Carbonation of Komatiite: Implications for H ₂ â€Rich Hydrothermal System and Ocean Chemistry in the Early Earth. Geochemistry, Geophysics, Geosystems, 2021, 22, e2021GC009827.	2.5	9
49	Chemical assessment of the explosive chamber in the projector system of Hayabusa2 for asteroid sampling. Earth, Planets and Space, 2020, 72, .	2.5	8
50	PIXE and microthermometric analyses of fluid inclusions in hydrothermal quartz from the 2.2Ga Ongeluk Formation, South Africa: Implications for ancient seawater salinity. Precambrian Research, 2016, 286, 337-351.	2.7	7
51	Heterogeneous nature of the carbonaceous chondrite breccia Aguas Zarcas – Cosmochemical characterization and origin of new carbonaceous chondrite lithologies. Geochimica Et Cosmochimica Acta, 2022, 334, 155-186.	3.9	7
52	Weak hydrothermal carbonation of the Ongeluk volcanics: evidence for low CO2 concentrations in seawater and atmosphere during the Paleoproterozoic global glaciation. Progress in Earth and Planetary Science, 2017, 4, .	3.0	6
53	Experimental chondrite–water reactions under reducing and low-temperature hydrothermal conditions: Implications for incipient aqueous alteration in planetesimals. Geochimica Et Cosmochimica Acta, 2022, 319, 151-167.	3.9	6
54	Tellurium stable isotope composition in the surface layer of ferromanganese crusts from two seamounts in the Northwest Pacific Ocean. Geochimica Et Cosmochimica Acta, 2022, 318, 279-291.	3.9	6

Τακάζο Shibuya

#	Article	IF	CITATIONS
55	Kinetics in thermal evolution of Raman spectra of chondritic organic matter to evaluate thermal history of their parent bodies. Meteoritics and Planetary Science, 2020, 55, .	1.6	5
56	Organic matter in carbonaceous chondrite lithologies of Almahata Sitta: Incorporation of previously unsampled carbonaceous chondrite lithologies into ureilitic regolith. Meteoritics and Planetary Science, 2021, 56, 1311-1327.	1.6	5
57	Exploration of Enceladus^ ^apos; Water-Rich Plumes toward Understanding of Chemistry and Biology of the Interior Ocean. Transactions of the Japan Society for Aeronautical and Space Sciences Aerospace Technology Japan, 2014, 12, Tk_7-Tk_11.	0.2	5
58	Enceladus as a potential oasis for life: Science goals and investigations for future explorations. Experimental Astronomy, 2022, 54, 809-847.	3.7	5
59	Thermodynamic Constraints on Smectite and Iron Oxide Formation at Gale Crater, Mars: Insights into Potential Free Energy from Aerobic Fe Oxidation in Lake Water–Groundwater Mixing Zone. Minerals (Basel, Switzerland), 2021, 11, 341.	2.0	4
60	Petrology of Peridotites and Related Gabbroic Rocks Around the Kairei Hydrothermal Field in the Central Indian Ridge. , 2015, , 177-193.		4
61	Elemental dissolution of basalts with ultra-pure water at 340°C and 40 Mpa in a newly developed flow-type hydrothermal apparatus. Geochemical Journal, 2013, 47, 89-92.	1.0	3
62	Removal of organic contaminants from iron sulfides as a pretreatment for mineral-mediated chemical synthesis under prebiotic hydrothermal conditions. Geochemical Journal, 2017, 51, 495-505.	1.0	3
63	Chemical composition and K–Ar age of Phengite from Barrovian metapelites, Loch Leven, Scotland. Journal of the Geological Society of Japan, 2013, 119, 437-442.	0.6	2
64	Development of Hydrothermal and Frictional Experimental Systems to Simulate Sub-seafloor Water–Rock–Microbe Interactions. , 2015, , 71-85.		2
65	Experimental Simulations of Hypervelocity Impact Penetration of Asteroids Into the Terrestrial Ocean and Benthic Cratering. Journal of Geophysical Research E: Planets, 2020, 125, e2019JE006291.	3.6	2
66	Enceladus: Evidence and Unsolved Questions for an Ice-Covered Habitable World. , 2019, , 399-407.		1
67	Post-drilling changes in fluid discharge pattern, mineral deposition, and fluid chemistry in the lheya North hydrothermal field, Okinawa Trough. Geochemistry, Geophysics, Geosystems, 2013, 14, n/a-n/a.	2.5	1
68	Experimental Hydrogen Production in Hydrothermal and Fault Systems: Significance for Habitability of Subseafloor H2 Chemoautotroph Microbial Ecosystems. , 2015, , 87-94.		1
69	Ar–Ar dating for hydrothermal quartz from the 2.4 Ga Ongeluk Formation, South Africa: implications for seafloor hydrothermal circulation. Royal Society Open Science, 2018, 5, 180260.	2.4	0
70	Identification of paleomagnetic remanence carriers in ca. 3.47ÂGa dacite from the Duffer Formation, the Pilbara Craton. Physics of the Earth and Planetary Interiors, 2020, 299, 106411.	1.9	0
71	Characterization of groundwater chemistry beneath Gale Crater on early Mars by hydrothermal experiments. Icarus, 2022, 386, 115149.	2.5	0